Lights, Camera, Voltage: Inferring Electric Grid Voltage Using Image-Based Sensing

Sylvia Imanirakiza
University of Massachusetts Amherst
Amherst, MA, USA
simanirakiza@umass.edu

Alex Yen
University of California San Diego
San Diego, CA, USA
alyen@ucsd.edu

Pat Pannuto
University of California San Diego
San Diego, CA, USA
ppannuto@ucsd.edu

Jay Taneja
University of Massachusetts Amherst
Amherst, MA, USA
jtaneja@umass.edu

Abstract

The global imperative for a transition towards renewable sources of energy is generating a groundswell of innovation and investment. Electricity is the linchpin fuel for transition, and substantial sectors of economies are moving towards full electrification, which will put massive strain on electricity grids. The challenges of widespread electrification are compounded in developing regions particularly, where many grids already struggle to provide reliable and stable electricity supplies, already hampering economic growth and livelihoods. Utilities and regulators - facing high costs for installing power quality measurement sensors throughout grids - often lack sufficient grid monitoring data, inhibiting their ability to plan appropriate system upgrades. In this work, we introduce a distributed voltage monitoring technique that leverages camera images to estimate sustained undervoltage events and normal voltages supplied to electric lights. We conduct a combination of in-lab and *in-situ* experiments using different light bulbs, varying voltages, and image and signal processing techniques to develop a robust method for non-contact estimation of grid voltage state. We demonstrate voltage state estimates for an *in-situ* deployment in a variety of challenging settings, including effective detection of undervoltage events at a sensing distance of 84m.

ACM Reference Format:
Sylvia Imanirakiza, Alex Yen, Pat Pannuto, and Jay Taneja. 2026. Lights, Camera, Voltage: Inferring Electric Grid Voltage Using Image-Based Sensing. In *The 13th ACM International Conference on Systems for Energy-Efficient Buildings, Cities, and Transportation (BuildSys '26), June 22–25, 2026, Banff, AB, Canada.* ACM, New York, NY, USA, 11 pages. https://doi.org/10.1145/3744256.3812553

1 Introduction

A global push to mitigate climate change and restrict the rise in global temperatures to 1.5 degrees above pre-industrial levels has spurred a concerted drive towards energy transition [24]. This shift is pivotal in the broader effort to transform the global energy sector from reliance on fossil fuels to embracing zero-carbon sources, with a primary focus on reducing energy-related emissions[3]. However, emerging economies face the dual challenge of decarbonizing and electrifying energy use while simultaneously addressing the overarching goal of growing economies and livelihoods through expanded energy access [15].

Despite these ambitions, these regions encounter a myriad of challenges within their electricity grids, characterized by low electrification rates, high unreliability, and frequent power disturbances due to inadequate infrastructure[11, 38]. These shortcomings in the power sector act as a substantial impediment to long-term economic growth and human welfare. Consequently, these grids find themselves ill-equipped to navigate the impending technological disruptions associated with the transition to widespread energy storage, large-scale electric cooking initiatives, and the proliferation of electric vehicles.

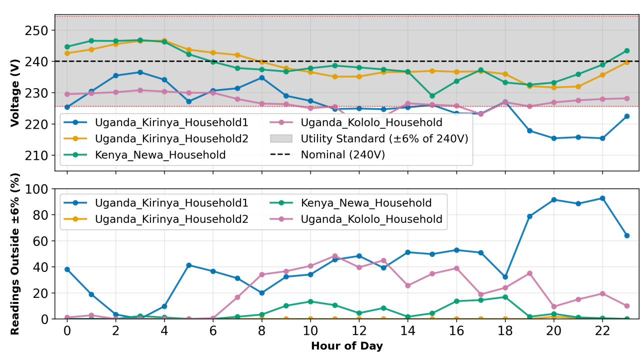

Figure 1: Voltage quality analysis across four sites in Kenya and Uganda over a 6-day period collected using plug-in voltage sensors. **(Top)** Average hourly voltage profiles for each of the four sites. The gray horizontal band indicates ±6% within nominal voltage (240V), the utility standard range for acceptable voltages. **(Bottom)** Hourly proportion of readings outside the utility standard. All sites exhibit undervoltage events, with the highest deviation rates during evening peak hours between 18:00 - 22:00.

Voltage quality, which is critical and influences the performance and lifetime of electronic equipment, remains under-measured, tracked and deprioritized by policies and standards. Researchers

BuildSys '26, Banff, AB, Canada

ACM ISBN 979-8-4007-2012-3/26/06
https://doi.org/10.1145/3744256.3812553

[8, 16, 23, 29] have only recently started to shed light on the underpinning complexities of voltage quality disturbances and the impact of these issues on economies and human welfare. Voltage disturbances, characterized by rapid fluctuations in voltage and sustained undervoltages or overvoltages, have been shown to cause electronic equipment to malfunction and sustain damage [25]. Figure 1 shows voltage traces from the deployment sites that illustrate the significant fluctuations reinforcing the case for granular measurement and monitoring of the electricity in such regions.

Monitoring voltage fluctuations informs the verification of quality of service, grid operations and maintenance [7]. For utilities particularly in low and middle-income countries, monitoring focuses on critical backbone areas, transmission interfaces (132 kV to 11kV), and interconnectors (220kV and 400kV), including cross-border links without special consideration for sensitive loads and large disturbance pollution sources [38, 40]. This dearth of sensing infrastructure further compounds the complexities faced by these regions as they strive to align with global energy transition objectives [32, 35]. Widespread measurement using modern computational techniques can enable better system planning and allow utilities to adapt and plan for the impacts of the energy transition [18, 20, 32]. Therefore, this motivates the need for spatially and temporally granular measurements to enable comprehensive mitigation of abnormal events.

Main Contributions: In this work, we present a first-of-a-kind method for estimating voltage state using machine vision cameras. We: (1) present proof of concept analysis through in-lab experiments using phototransistor-based capture of light bulb behavior to establish the relationship between the lighting behavior while step-wise varying supply voltage (Section 4.1); (2) deploy the camera-based system for monitoring the electric grids across different sites and observing bulbs in outdoor real-world settings with varying power quality conditions (Section 4.2).

Our paper makes the following novel contributions:

- Through in-lab experiments using phototransistor-based and camera-based capture of bulb behavior, we identify the maximum, minimum, mean, median, signal energy, and peak-peak features of the bulb response functions, as highly indicative parameters exhibiting high absolute correlation with the voltage changes across bulbs and bulb types. We show that these observations are consistent across a variety of bulbs.
- We demonstrate a technique using off-the-shelf hardware components and signal processing techniques for collecting a clean (low noise) bulb response function that is able to work in real-world settings at a significant distance (over 80m).
- We develop a machine learning-based method for classifying collections of captured images as within or outside of acceptable voltage ranges.

2 Motivation and Related Work

In this section, we provide background on power quality monitoring approaches and their shortcomings as well as make a case for the development of high resolution voltage monitoring techniques.

2.1 Traditional Power Quality Monitoring

Traditional approaches to power quality monitoring relied on specialized instruments for individual parameters [7]. The use of smart metering infrastructure has become a conventional choice for monitoring power quality as it integrates data from all available intelligent devices in the smart distribution grid, while adhering to international standards (e.g. IEC 61000-4-30). Despite these advancements, the sector face a number of constraints, including low deployment coverage [42], high costs of procuring and installing smart metering infrastructure [13], communication barriers caused by insufficient fiber optic and 4G/5G penetration [5], and the data limitations and computational challenges for optimizing monitor placement.

In particular, the adoption of smart meters in Sub-Saharan Africa is still in its nascent stages [31]. Some countries have made limited strides in the rollout and transition to advanced metering infrastructure necessary for enhancing energy access, regulatory oversight, and innovation. In 2023 and 2024, Kenya announced the procurement of over 500,000 smart meters [1, 26]. Eskom, South Africa's leading electricity utility, has established a number of phased rollouts of advanced metering infrastructure for large power users and domestic customers. The deployments are focused around a few municipalities in the cities of Johannesburg, Tshwane, and Nelson Mandela Bay [6]. However, deployment of advanced metering infrastructure across the region remains scant, especially among non-industrial customers.

2.2 The Need for High Resolution Grid Monitoring

Researchers have documented power quality challenges typically by temporarily deploying traditional or purpose-built metering systems [8, 32]. To address the need for granular and continuous spatial and temporal measurements of grid operations, academics and industry practitioners across energy and communication domains have shown intelligent alternative techniques to improve the monitoring and observability of electric grid dynamics. The GridMetrics Platform [20] by CableLabs features over 300,000 deployed broadband based power sensors that are deployed across the US. The real-time data is ingested, audited, analyzed (in 5 minute intervals), and transmitted via broadband while leveraging the close interaction of electric transmission lines and fiber optic communication systems. Another similar platform is nLine's GridWatch technology [18], which features remote power quality via PowerWatch monitoring sensors that measure RMS voltage every 2 minutes when plugged into the power outlets of homes, businesses, and others. Real-time data are transmitted via a cellular network with local data storage to protect against network interruptions. While such advancements present significant progress in improving the monitoring of grids by utilities and regulators, mass deployment of these technologies requires significant financial investment from stakeholders.

2.3 Side-Channel and Computational Imaging Techniques

Side-channel measurement techniques have gained interest as a method to enable high-resolution monitoring of electricity grids, particularly at the grid edge of customers. Bianco et al.[10, 14] demonstrated that hypertemporal imaging of an urban lightscape can aid in observing and detecting the dynamics of the electric grid—particularly phase changes—on varying time scales with a granularity to the individual housing unit. They employed a digital camera and a special liquid crystal shutter to observe light sources across the NYC skyline. Breda et al. [12] developed a system that uses only a commodity smartphone and a consumer fan to measure the voltage of an electricity grid. They leverage the microphone of the phone to measure the perturbation created on a pure sinusoidal tone into a running fan. The distance between adjacent harmonics in this disturbance acts as a proxy for the grid voltage.

In relation to computational imaging, different researchers have exploited computational imaging through conventional shutter-based cameras and event-based cameras for detecting and estimating electrical network parameters. Sheinin et al.[36] first proposed a novel coded exposure mechanism that demonstrated how grid dynamics can be observed and derived a bulb response function that characterises the electricity supply. Xu et al. [39] proposed the use of an event-based camera that collects the illumination changes and converts them into an event stream for frequency monitoring. Using the methodology proposed by [37], Shah et al.[35] later proposed a group of side-channel techniques for monitoring of grid parameters like phase, frequency, and voltage using a method developed by Sheinin et al. [37] for leveraging the rolling shutter effect in digital cameras to capture light bulb response functions. One limitation of the system by Shah et al. is that the voltage measurement was performed in a highly controlled setting yet still had substantial errors in voltage estimation with a measurement error of nearly 15%.

In comparison to prior work, our work presents techniques that leverage conventional rolling shutter-based cameras to measure electric grid voltage by direct observation of light bulbs. To validate the efficacy of the system, we first establish proof of concept evaluation based on in-lab experiments that set the stage for inferring the patterns of behavior relating the bulb response functions and voltage quality variation. Then, we carry out *in situ* experiments to validate the feature patterns and design machine learning-based techniques for predicting the voltage level of the supply. These validate and measure the effectiveness of estimating the grid voltage level using these techniques in the presence of environmental factors and unknown bulb types.

2.4 Deployment Cost Considerations

To provide further quantitative motivation for the cost-effectiveness of this proposed approach, we analyze the deployment requirements for image-based voltage sensing.

Using 3D building footprint data [43] from Kileleshwa, a residential neighborhood in Nairobi, Kenya, we identify candidate deployment areas based on building density and height distributions (top left on Figure 2). We note that this neighborhood contains a mix of high-rise and low-rise buildings. We then apply a greedy set-cover algorithm to determine the minimum number of camera placements needed to achieve varying levels of building coverage, targeting camera deployments to high-rise buildings (i.e., those with height greater than or equal to 20m). The top right of Figure 2 illustrates a sample deployment plan where 11 strategically-placed camera sites can monitor 149 target buildings within their coverage radii of 75m. Consider that each camera site hypothetically requires 3 cameras for 360° coverage at $300/camera.

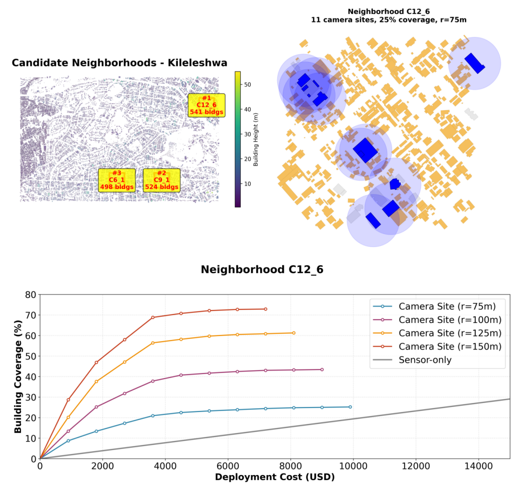

Figure 2: Camera-based deployment cost analysis for voltage monitoring in Kileleshwa, Nairobi. **(Top Left)** Building height map with candidate 500m×500m neighborhoods identified by grid-based suitability scoring. Red boxes indicate the top three neighborhoods ranked by camera deployment potential (buildings greater or equal to 20m) and target coverage (buildings less than or equal to 15m). **(Top Right)** Optimal camera placement for neighborhood C12_6 using a greedy set-cover algorithm with 75m coverage radius. Blue triangles mark selected camera sites on high-rise buildings; blue circles show coverage zones; orange buildings are monitoring targets. **(Bottom)**Cost-coverage comparison showing camera-based deployment (colored curves for different coverage radii) versus sensor-only deployment (gray line). Each camera site requires 3 cameras for 360° coverage at $300/camera; sensors cost $100/unit. Camera deployment achieves 25%+ coverage at roughly $5,000, while sensor-only deployment would exceed $12,000 for equivalent coverage. Improved image resolution enhances the cost difference.

The bottom of Figure 2 presents the cost-coverage tradeoffs for camera-based monitoring versus plug-in voltage sensors. Our analysis shows a characteristic saturation behavior in the camera deployment curve: initial deployments yield high marginal coverage gains as cameras on tall buildings can observe multiple targets simultaneously, but saturates as optimal camera vantage points become exhausted. In contrast, the plug-in sensor approach scales linearly with coverage targets, as each additional building requires its own dedicated sensor installation. At a coverage radius of 100 meters, approximately 30% of target buildings can be monitored with camera deployment costs of approximately $3,000, whereas achieving equivalent coverage through individual plug-in sensors would require over $15,000, a 5× cost difference. Prior work has demonstrated a similar spatial multiplexing advantage of camera-based sensing, where a single elevated vantage point can simultaneously observe numerous buildings; i.e., Bianco et al. [10] captured

1,533 light sources from a single camera location in Brooklyn, NYC, illustrating the substantial monitoring reach achievable from one well-positioned sensor. Further, rapid improvements in image resolutions can augment the difference in coverage. Note that this analysis does not include installation costs, which are likely to be appreciably higher for in residence installations.

Important to note, utilities need not achieve complete building coverage to derive operational value from grid monitoring. The saturation curve suggests that a targeted deployment strategy, focusing on high-value vantage points, can achieve useful coverage at a fraction of the cost of comprehensive sensor rollouts, with the flexibility to expand incrementally as monitoring and technology needs evolve.

3 Technical Background

This section provides a primer on computational imaging of the grid techniques relevant to our work.

3.1 Flickering of Alternating Current Lighting

For most electric grids, electric power is distributed to consumers in the form of alternating current (AC). Usually electricity is delivered in three phases and a customer is typically tapped on a specific phase (or depending on their power requirements, all three phases). The AC voltage supplied can be represented as:

$$V(t) = (\sqrt{2} * V_{\text{rms}}) \sin(2\pi f t - \phi)$$

where ϕ is the phase of the wave, f is the frequency, and V_{rms} is the root mean square voltage that can be 120 V or 240 V, depending on the grid. The voltage oscillates at a frequency f, which can be 50 or 60 Hz depending on the country. For the bulb connected to the system, it is supplied by a mains with a voltage of $V(t)$. Following from the modeling and abstraction in prior work, the bulb flickers at double the grid frequency. This flickering behavior has a period that we define as:

$$\Delta = \frac{1}{2f}$$

This behavior is mediated by various mechanisms and influenced by the internal circuitry of the bulb system. As demonstrated in prior work [35, 36], a photodiode placed near a bulb can be used to record timely measurements to give the bulb response function (BRF), as illustrated in Figure 3. This forms the basis of our in-lab experiments where we create our own dataset of BRFs of different bulbs under varying voltages, which is discussed in more detail in Section 4.1.

3.2 Rolling Shutter Imaging Model of Light Flicker

Given the speed of the flicker and manufacturer specifications, this flicker is usually too subtle and fast for the naked eye to notice. In practice, the flicker behavior of lights is monitored and measured using flickermeters that are usually standardized based on the incandescent lamp [30]. These systems are modelled in such a way to quantify the level of irritation observed by humans in response to the flickering of the lamp following the IEC 61000-4-115 standard [30]. Additionally, photography and computer vision applications find the flicker as a nuisance due to the introduced banding artifacts and motion blur [21]. Nonetheless, this flicker has enabled different use-cases including understanding grid behavior [10, 37, 39]. Owing to the influence of the internal circuitry of the bulb system, prior work has shown to enable fingerprinting capabilities of a particular bulb type's light flicker from AC [41].

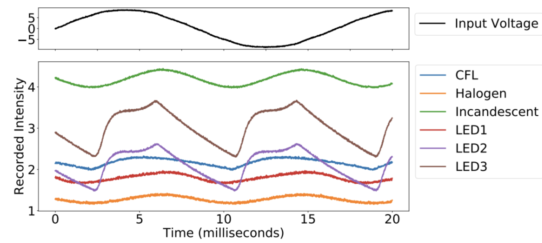

Figure 3: Bulb Response Functions of different bulbs recorded using a phototransistor and an oscilloscope. The distance between each bulb and phototransistor is identical (i.e. 40cm). Signal recordings are triggered at the zero crossing of input AC voltage waves on the oscilloscope (reprinted with permission from [35], © 2019 Association for Computing Machinery).

Prior work by Sheinin et al. [36, 37] proposed methods to observe and derive the flickering behavior of bulbs in the form of bulb response functions (BRFs). The BRF is a unit-less, temporal function that expresses a light bulb's luminosity response to the input AC voltage. In both works, Sheinin et al. and Shah et al. present a rolling shutter model for a bulb's light response to an AC flicker. When an AC-electricity illuminated scene of light bulbs is viewed by a rolling shutter camera, the sequence of captured rolling shutter frame expresses a spatiotemporal wave function that moves vertically with an upward velocity. During this capture, the sequence of frames in raw form lacks synchronization with the input AC-electricity. However, different methods are proposed to accurately synchronize image measurements (frames ordering) to the grid's electricity behavior.

In this paper, we directly, and only, rely on information from a scene consisting of grid-powered light bulbs without external or prior information to estimate that bulb's underlying voltage fluctuation. In this case, we maintain the presence of a diffused surface in the scene reflecting light to the camera. The light shone on this diffused surface serves as a reference bulb. Following from the surface-based method [37], we capture a sequence of rolling shutter frames at an exposure duration less than the period within the flicker cycle (1/2f). Additionally, we capture the image when the exposure time is set to the period of the flicker or its integer multiple; the image captured is unaffected by the flicker pattern of the sources illuminating the scene and represents imaging under direct current (DC) electricity. In this method, a derived DC-based image is optional and can be approximated. In our experiments, we automate this and capture the DC image.

4 Methodology

In this paper, our main goal is to investigate the relationship between bulb response functions (BRFs) and grid voltage, with the aim of validating and evaluating the proposed system under different

Table 1: Summary of how the proposed image-based, voltage sensing system is evaluated across experimental settings. The intuition in the sensing and processing pipeline (light source → BRF capture → feature extraction → pattern recognition) are analogous; with only the environment and capture conditions differing.

Experiment	**In-Lab** [Section 4.1]	**In-Situ** [Section 4.2]
Light Source	Controlled bulbs on testbench	Building-mounted lighting in urban scene
Distance from acquisition setup	approx. 3-10 inches (dependent on brightness)	<40 m (Kenya site) / 84 m (Uganda site)
Acquisition Device	Phototransistor + oscilloscope	IDS rolling-shutter camera
BRF duration	20.833 ms (two and a half cycles)	10ms (a single cycle)
Voltage Variation	Stepped 80–130 V (10 V increments)	Observed occurring instantaneous voltage fluctuations with 2 minute resolution
Ground Truth	Stepped transformer output	Plug-in PowerWatch voltage sensor
Research Question	RQ1	RQ2

operating conditions and environments. To achieve this, we posed the following research questions:

RQ1. Are there patterns in intensities that can be exploited to help predict voltage across a range of different bulbs? [Section 4.1]

RQ2. Can image-based sensing of BRFs feasibly detect changes in grid voltage state? [Section 4.2]

Table 1 provides a high-level description of the experimental design we follow to answer these questions.

4.1 In-lab Experiments

The primary goal of the in-lab experiments is to demonstrate the feasibility of inferring grid voltage from bulb response functions (BRFs) under controlled conditions. We employed an oscilloscope-phototransistor setup to capture the fluctuations in light emitted by various bulbs under different voltage levels.

BRF acquisition: To capture the fluctuations in light emitted by a bulb of interest, we follow the acquisition approach for extracting BRFs proposed and used by prior work [35, 36, 41]. Sparkfun's TEMT6000 is used to sense the BRFs by converting incident luminous flux into a voltage reading. This allows the sampling of the analog intensity of light from the bulb powered by an AC voltage supply. The voltage readings from the phototransistor are sampled through an oscilloscope. For each bulb, we trigger the synchronous capture of 200 different instances of two and a half cycle waveforms, each instance comprising of 2000 data points. We collect data for 11 randomly selected bulbs with different bulb types and wattage characteristics (5 LEDs, 3 Incandescents and 3 CFLs). Analogous to prior work by Shah et al. [35], each waveform's recording is triggered on the rising edge at the zero crossing of the power supply voltage in order to maintain consistent readings. To measure and analyze how a BRF reacts in response to varying voltage, each bulb is plugged into a stepped transformer that is adjusted from 80V to 130V in 10V increments.

Data analysis and cleaning: Capturing BRFs using a phototransistor provides high resolution data due to the flexibility in terms of sampling rate. However, a limitation of this method is that it generates significantly noisy signals. To reduce noise and generate clean BRFs that are sufficient for voltage analysis, we average corresponding data points across all 200 samples for each voltage level. The resulting clean waveforms were stored in a lighting dataset for further BRF analysis. The BRFs for three different bulbs from each bulb type in our dataset are shown in Figure 4a. This dataset enables us to answer whether light intensity patterns via BRFs can enable grid-voltage-level predictions in a controlled setting.

4.2 In-situ Experiments

In the in-situ deployment strategy, we move away from controlled, in-lab experiments to outdoor experiments, in which the outdoor setup supersedes the oscilloscope-phototransistor setup with camera equipment deployed in the wild, set-up as shown in Figure 5. The experiments were conducted in two geographical locations as summarized in Table 2, one in Uganda for 3 consecutive days and another in Kenya for 6 consecutive days; both sites' grids operate at 240V/50Hz.

BRF acquisition: For the in-situ experiments, we use IDS Vision's UI-3860CP-M-GL Rev.2 monochrome camera [4] with a mounted near range, wide field of view camera lens, the Fujinon HF9HA-1B 9mm f/1.4. The vision camera possesses a 2.1 MP CMOS sensor (IMX290), providing a resolution of up to 1936x1096 pixels.

For further detail, we refer to the approach proposed by Sheinin et al. [37] for capturing BRFs using surface-based and emitter-based capture. The camera was operated using an exposure time (i.e. reciprocal of shutter speed) of 3 ms for the rolling image sequence and 1/120 for the dc image, gain of 0 dB. We use the vision camera to directly monitor the light bulb and extract BRFs. Using the algorithm in [37], the camera is calibrated to record at a certain frame rate depending on the grid frequency. In this scenario, the frame rate is set to 49 fps with exposure times between 1ms-5ms. As such, the rolling shutter camera is essentially sampling different points of the signal temporally over time. The frame rate mismatch (49.5 Hz vs. 50 Hz) leads to a gradual temporal offset across K = 80 frames. This causes each new frame captured to sample the scene as a slightly different point in the light flicker cycle, and, consequently, the AC cycle. The exposure time is set short enough to capture variations in brightness due to rolling shutter effects. By correctly ordering

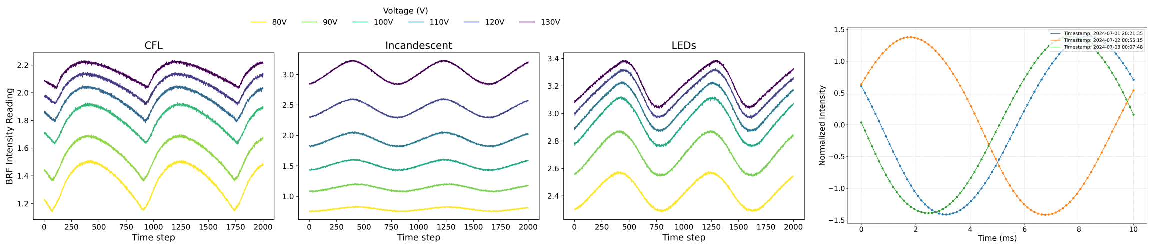

(a) **(b)**

Figure 4: (a) Photo transistor-captured Bulb Response Functions for three different bulbs of three types: CFL, Incandescent, and LED. For each bulb, the different curves represent its response over time for six corresponding voltage levels ranging from 80V to 130V. Lighter and darker curves represent lower and higher supply voltages, respectively. Each waveform corresponds to two and a half AC cycles,and **(b) Three samples of Bulb Response Functions recorded using a rolling shutter camera deployed during the in-situ experiment for the site in Uganda**.

the 80 collected frames, the algorithm recovers a canonical representation of the AC cycle's impact on lighting, thus reconstructing a globally synchronized timeline for the light flicker, giving the interpolated bulb response function within a cycle. Postprocessing is performed to extract the temporally aligned pixel intensity over time relations, and this reconstructs the BRF.

For both sites, the camera is set up in a building overlooking a scene containing the bulb(s) of interest, as depicted in Figure 5b, which shows the camera point of view. To accommodate significant distances and different scene intricacies, we consider 3 different exposure durations ranging from 1ms to 5ms, provided they remain shorter than the flicker period, which is the reciprocal of twice the grid of interest frequency of operation (in this case, 10ms). The in-situ experiments are set up in such a way that the data collection period spans 11 hours from 7pm to 6am (i.e., when lights are turned on), with a granularity of 5 minutes for each exposure with a delay of a few seconds to allow camera settings to reset. In the Kenya deployment, the light bulb that we monitor is less than 40m from the camera location. In the Uganda deployment, for our analysis and BRF extraction, we observe and monitor a light bulb attached to a building in the scene that is 84m away from the camera as shown in Figure 5a.

Pixel selection: In prior work, Shah et al. [35] and Yen et al. [41] manually select pixels of interest to focus and extract a BRF based on qualitative analysis. This approach has certain flaws that are impermissible for our analysis: it is highly observer dependent and prone to human error; selections on arbitrary pixels may fall within a heavily saturated region, resulting in information loss; manual pixel selection ignores data provided by other regions of the bulb that may be relevant to characterizing intra-frame variability and thus the overall reliability and repeatability of a BRF measurement.

Therefore, we propose an image processing-based framework for pixel selection. Shown by Sheinin et al. [37] and Shah et al. [35], this framework leverages the grayscale DC image, which is derived and first cropped to focus on the light bulb in the scene. We adopt the Laplacian of Gaussian blob detection method, originally proposed by Marr and Hildreth [22] using the scikit-learn library implementation. We iterate and set the key parameters of max_sigma to 100 to define the upper bound of the kernel sizes, and num_sigma set to 10

Table 2: Summary of the in-situ deployments at two sites, in Uganda and Kenya

Country	Duration	Number of datapoints	Relative distance between bulb and camera
Uganda	3 days	347	84m
Kenya	6 days	650	<40m

to control the number of intermediate scales evaluated within this range. Additionally, we select a threshold value of 25 to eliminate weak responses and preserve the most significant blobs related to the light bulb. To ensure reliability for our subsequent analysis, we manually inspected the results to ensure consistency and identify potential false detections, correcting for the few scenarios where misalignment occurs. Compared to other blob detection methods like the difference of a Gaussian and determinant of a hessian, we found that the Laplacian of a Gaussian was the more suitable option owing to its scale invariance, limited complexity, and simplicity. We leave the investigation of more sophisticated and fully automatic methods to future work.

Ground truth Voltage measurements: To establish ground truth measurements of grid voltage levels, we install plug-in voltage sensors within buildings close to the bulb(s) of interest that the cameras observe. These sensors are installed in the power outlets of the household which is connected to the same power line as the observed bulb. The plug-in voltage sensors record and provide measurements in 2 minute intervals. This interval adequately captures common low frequency variations in voltage. Figure 5a illustrates the set-up showing the relative locations of the ground truth PowerWatch sensor [19, 28], the camera and the bulb observed.

5 Analysis

5.1 In-lab Experiments

Feature Extraction: In order to describe and characterise the pattern between the bulb reference functions and the supply voltage variations, we apply manual feature extraction to transform the signals into meaningful fingerprints. Based on domain-specific knowledge, we extract features that describe each BRF signal based on time domain statistical analysis [17]. The intensity of a bulb is

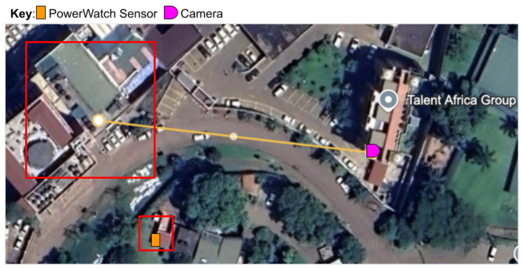

(a)

(b)

Figure 5: (a) Experimental setup for the in-situ study in Uganda. It shows the relative positions of the camera, the ground-truth plug-in voltage sensor, and the observed light bulb. **(b)** Photograph depicting the camera setup deployed on a high-rise building, positioned to monitor the target bulb in the in-situ experiments.

dependent on the input AC voltage and the bulb type [36]. As such, given that our interest is with distinguishing the source AC voltage for each bulb, we hypothesize that amplitude-related features will provide a more direct focus on the intensity variations with voltage from the source irrespective of bulb type. The eight features extracted in our work are as follows: mean, median, peak-to-peak, kurtosis, skew, maximum, minimum, and signal energy. The mean and median show the central tendency of the signal. The peak-to-peak captures the statistical dispersion by finding the difference between the maximum and minimum. The kurtosis and skewness typically measure the asymmetry and the sharpness of the peak of the signal distribution. The maximum and minimum track the amplitude/peak value variations across different signals. The signal energy measures the signal strength, intensity, and energy content. In terms of electric signals, it is analogous to the total energy of the signal dissipated over a 1 ohm resistor [33].

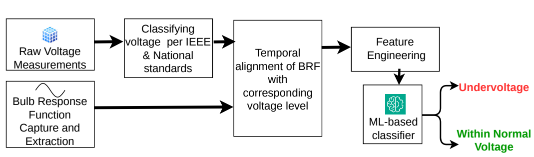

Figure 6: Overall analysis workflow for the in-situ experiments.

Pattern Recognition: With the features, in order to uncover the pattern for each bulb type, we perform a correlation analysis between the voltage and BRF extracted features for the different bulbs.

5.2 In-situ Experiments

The overall system analysis workflow for the in-situ is shown in Figure 6.

Matching BRF measurements with ground truth. To combine the measurements on a temporal scale for labeling, we filter the data to isolate data from the sensor that was closest to the bulb being monitored. Subsequently, the sensor data were constrained to the time window corresponding to the camera observations. To combine the image sequences and the sensor readings, we match each voltage reading to the rolling-shutter image sequence taken within 1-2 minutes of the voltage reading. Recall that in the in-lab experiments, the controlled voltage steps were 10V, however, voltage fluctuations in the real world exhibit smaller and granular changes on the order of +/- 1V and above over time, as shown in the voltage profiles for these sites as seen in Figure 1.

Feature Engineering and Supervised Learning. A main contribution of this work is to predict the voltage level for a scene based on the lighting fingerprints. For each site, the voltage measurements had many instances of undervoltage but no instances of overvoltage within our duration of deployment. We implement and compare three different machine learning approaches [27]: K-Nearest Neighbours (k-NN), Random Forest (RF) and Decision Tree (DT) to detect whether scenarios within the normal operating voltage or undervoltage. In practice, this approach will detect brownouts or undervoltage events. The threshold for undervoltage is defined based on local and international voltage quality standards, such as IEEE 1159 [2, 34]. For Uganda and Kenya [2], the voltage tolerance limit of a single-phase supply is +/- 6% of nominal voltage, labeling voltages below 226V as undervoltage and within the tolerance range as normal voltage.

As described in Section 5.1, we extract the eight features for every BRF in each dataset. These features are used as training variables, and the corresponding label, of normal voltage or undervoltage. For each dataset, we apply a 70/30 split, where 70% of that particular dataset is used for training and the rest is held out for testing.

We employ 3-fold grid search cross-validation for hyperparameter tuning and exhaustive combinatorial search across all possible feature combinations ranging from 3 to 8, totalling 219 possible feature subsets to identify the optimal feature subset and optimal parameters per model. Using the best parameters and feature subset in Table 3, we train and implement the three models separately for the datasets collected from Uganda and Kenya respectively and evaluate their performance.

6 Results

We first analyze and discuss results with respect to our in-lab, oscilloscope-based setup, which then set up the precursor information to perform voltage model prediction in our in-situ experiments.

6.1 In-lab Experiments

As discussed in Section 5.1, to gain an understanding of the patterns uncovered through the features we extracted for the in-lab

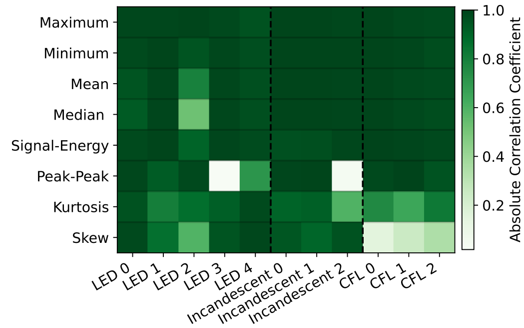

Figure 7: Absolute correlation coefficients between the features extracted from each bulb and voltage changes in the in-lab oscilloscope dataset. The y-axis represents all of the extracted features we use in our study, and the x-axis represents the various bulb types we use to correlate the extracted features with voltage. Each label on the x-axis represents the bulb type along with a unique manufacturer and wattage. In general, the bulb's wattage rating is increasing with respect to the index (e.g. wattage of LED 4 > LED3 > ... > LED 0).

oscilloscope dataset, we first present the results of this analysis. Using Pearson's correlation, we compute the correlation coefficients for the feature of each bulb with respect to voltage changes. The degree of variation is consistent for a bulb but differs by bulb. Figure 7 shows a detailed overview of the coefficients with respect to various tested bulbs. This figure elucidates two questions: (1) how generalizable are certain features to work across a wide variety of different bulbs, and (2) are there indications that particular bulbs in-the-wild will not exhibit strong correlations between features and voltage?

To start, we discuss the correlation between features and voltage. From the top-down, the maximum, minimum, mean, median, signal energy, and peak-peak range, exhibit strong correlation with the voltage changes across bulbs and bulb types. In particular, the maximum, minimum and signal energy have absolute correlation coefficients close to 1 for all of the bulbs, indicating that these features have the desirable property of varying similarly to the supply voltage. While other parameters like peak-peak, kurtosis, and skew have high correlations for many bulbs, their inconsistency and occasional low correlations make them less attractive for our purpose of voltage estimation. As such, Figure 7 underscores the importance of designed and selected features that yield a strong and direct correlation with voltage.

We then observe how particular bulbs fair with respect to features. "LED 2" particularly struggles with respect to the median and mean features even though the rest of the selected bulbs do not exhibit weaker correlations. This emphasizes the fact that particular bulbs may not produce an analyzable BRF in the real world, which we must be aware of. From this information, we must be cognizant about verifying that whatever bulb we select to analyze must yield a BRF such that extracted features show a markedly observable correlation with voltage. This concern is further discussed in Section 7.2.

6.2 In-situ Experiments

In these settings, the BRFs are captured using the deployed camera as described in Section 5.1. As a major finding in this work, we show a remarkable waveform reconstruction for the flicker waveform for a directly observed bulb over 80m away, as illustrated in Figure 4b.

As described in Section 5.2, through an exhaustive feature combination search, we determine the optimal feature combinations for each classification model for the sites, as shown in Table 3. In general across all cases, the top features that occur as important for different classification models and sites, are maximum, minimum, mean, peak-peak. This is consistent with the finding observed in the in-lab case. Considering the site specific scenario for the Uganda dataset, there exists variability in the best performing feature combination across models. On the other hand, the feature combination remained consistent for the Kenya dataset.

For evaluating performance of the models, we use macro-average accuracy, F1 score, precision, and recall. Accuracy measures the proportion of correctly classified instances out of the total number of objects in the dataset, which is the ratio of correct predictions to the total predictions made by the model. Precision evaluates the model's ability to correctly identify instances of a particular class, while recall measures the model's ability to capture all instances of that class. The F1 score is the harmonic mean of the precision and recall. Macro-averaging gives equal weight to each class, regardless of the class distribution in the dataset, providing a balanced evaluation of performance across all classes.

Table 3: Best-performing feature combinations and tuned hyperparameters for each classification model by dataset. UG: Uganda; KY: Kenya; k-NN: k-Nearest Neighbors; DT: Decision Tree; RF: Random Forest.

Site	Model	Best Features	Best Parameters
UG	k-NN	maximum, minimum, median	`n_neighbors=7`
	DT	maximum, minimum, mean, skew	`max_depth=3, min_samples_split=10`
	RF	minimum, mean, peak-peak, median	`max_depth=None, n_estimators=50`
KY	k-NN	maximum, mean, peak-peak	`n_neighbors=5`
	DT	maximum, mean, peak-peak	`max_depth=7, min_samples_split=5`
	RF	maximum, mean, peak-peak	`max_depth=7, n_estimators=50`

Table 4 shows a comparison of the performance of the different models. Across all the considered metrics, the Random Forest (RF) model demonstrates overall better and more consistent performance across the two sites, with an accuracy of 94.9%, precision of 94.7%, recall of 89.8% and F1 score of 92.0% for the Kenya dataset, which outperforms the other models. For the Uganda dataset, while all three models achieve similar accuracy of 91.4%, the RF achieves better recall and F1 score than the DT and k-NN. Recall and F1 are particularly important for our use case given the imbalance of our dataset having fewer undervoltage scenarios. We would prefer a model that is capable of better isolating the undervoltages.

Table 4: Comparison of the performance of different models trained and evaluated on datasets from the Uganda and Kenya sites using a 70%:30% train–test split.

Site	Model	Accuracy	Precision	Recall	F1
UG	k-NN	**0.914**	**0.890**	0.804	0.838
	DT	**0.914**	**0.890**	0.804	0.838
	RF	**0.914**	0.873	**0.825**	**0.846**
KY	k-NN	0.923	0.889	0.882	0.885
	DT	0.938	0.939	0.874	0.902
	RF	**0.949**	**0.947**	**0.898**	**0.920**

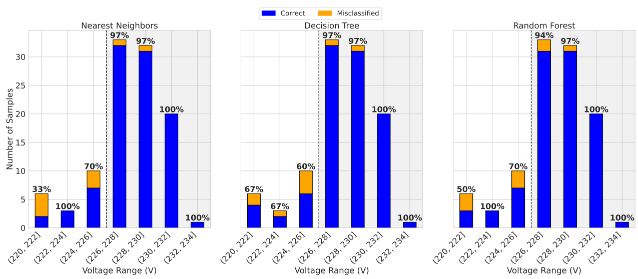

(a) Uganda

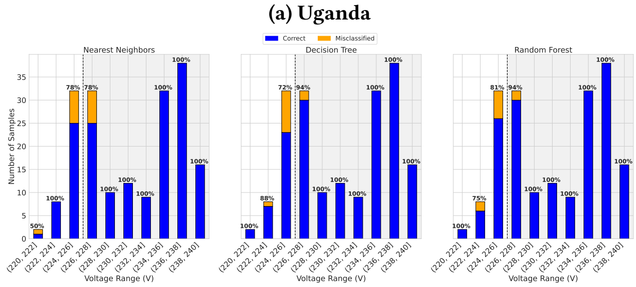

(b) Kenya

Figure 8: Classification results for normal and undervoltage observations and predictions for Uganda and Kenya. For each figure, a vertical line is annotated at 226V to signify the normal and undervoltage threshold, such that under 226V is undervoltage and over 226V is normal voltage. As such, any orange under 226V indicates that the model misclassified as normal voltage, and any orange above 226V indicates misclassification as undervoltage.

To examine further nuances about model performance, we analyze the distribution of the binary predictions with respect to PowerWatch's ground truth voltage readings. Figure 8 presents the performance of the k-Nearest Neighbors, Decision Tree, and Random Forest models in detecting voltages levels from light bulbs in the Uganda and Kenya sites. Generally, each model performs well to accurately classify instances of undervoltage (brown-out) and normal voltage instances. However, as expected, confusion occurs at the threshold, in which models are more likely to confuse undervoltage with normal voltage predictions. For each model with respect to each dataset, we can observe misclassifications right at the cutoff between normal and undervoltage (i.e. 226V). For the misclassifications in the Uganda dataset, we observe a higher misclassification rate for undervoltage classifications in each model versus normal voltage classifications. This may be attributed from model perceiving the BRF as though it were operating in a normal

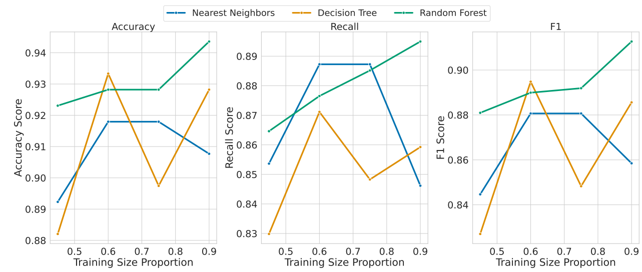

Figure 9: Performance metrics (accuracy, precision, recall, and F1 score) for the three models as a function of varying training dataset sizes. Each subplot illustrates one of the metrics.

voltage condition versus an undervoltage condition, owing to the majority of the edge cases lying within the normal voltage range. Results from each model indicate that the threshold value is indeed difficult for a model to distinguish whether a bulb's underlying power supply is at normal voltage or undervoltage. However, this is less the case in the Kenya dataset, where there is a fair balance at the margin, and the model is able to maintain accuracy.

Considering the extreme cases of undervoltages in the Uganda dataset, for the decision tree and random forest are able to atleast correctly classify occurences when ground truth is 220=222 V, as correctly undervoltage with an accuracy of 67% and 50%. Overall in classifying the undervoltages occurences, the random forest performs better on average. Similar trend is observed in the case of the the Kenya dataset. Additionally, for the Kenya dataset, we evaluate the model's performance under varying training dataset sizes, as shown in Figure 9. The results highlight the consistent reliability of the Random Forest (RF) model for this task. These findings suggest that the approach could achieve significantly improved performance with access to larger training datasets and higher camera resolution, even when monitoring bulbs at substantial distances.

7 Discussion and Future Work

We discuss the implications, limitations, and future work with respect to our proposed methodology and system for voltage detection via cameras and visible light.

7.1 Implications

This research addresses a critical challenge in developing regions, where poor power quality experiences – particularly brownouts – significantly impact the usability of electricity [9, 23]. As electricity consumption rises due to the ongoing energy transition, this issue is expected to worsen. The proposed system offers several practical applications. First, it can be deployed statically on buildings to complement power quality mapping efforts, enhancing the accuracy and comprehensiveness of grid monitoring and enabling strategic upgrades. Second, it can assist in tracking energy access indicators, moving beyond mere counting of connections to assess the actual quality of electricity received by consumers.

In low- and middle-income countries (LMICs), per-site smart plug deployment is limited by connectivity, cost, and installation complexity. Our approach requires a single device per vantage point, covering multiple bulbs enabling spatial multiplexing that can reduce deployment costs by up to 4× compared to plug-in sensors (as shown in Section 2.4). On a larger scale, this can be integrated into city-wide urban observatory systems [14], providing critical insights for managing and improving urban energy infrastructure. The system is primarily oriented towards nighttime deployment when artificial lighting is used. Evening hours coincide with peak demand and significant voltage fluctuations in many LMIC grids [8, 16, 29], so night-focused monitoring captures periods of highest operational relevance.

7.2 Limitations

While the proposed system offers promising applications, we acknowledge limitations. First, the post-processing software of different cameras can significantly affect image rendering, potentially influencing measurement accuracy. This effect has not yet been studied in detail. Furthermore, camera sensors vary, and a camera measurement setup different from ours likely requires catered models and new data collection with respect to that setup. In addition to varying camera sensors, different scenes may require different lenses for the vision devices, adding complexity to deployment. The angle at which the system perceives the light source can also influence measurements, though this aspect has not been fully explored. Another limitation lies in the behavior of certain bulb types, particularly LEDs in our in-lab experiments and results. Not all LEDs exhibit a periodic waveform, which limits the ability to estimate the source frequency from flicker frequency. Other LEDs are just generally harder to characterize -this is more evident in Figure 7, in which the "LED2" does not exhibits a strong correlation between the selected features versus voltage in comparison to other LED, incandescent, and CFL bulb types. Our approach hinges upon the necessity for a definitive, periodic light signal. Lastly, privacy concerns are another consideration. While the current setup minimizes privacy risks by capturing only bright lights with small exposures and deploying devices out of the line of sight, additional security measures are needed to ensure data privacy and integrity, particularly for large-scale deployments.

7.3 Future Research Directions

Different factors including—but are not limited to—bulb wattage, luminous flux, aging of bulbs and other environmental factors (e.g., ambient lighting), as well as distance influence our system functionality because they likely affect the viability of data collection; if our camera perceives a light to be too dim, a proper BRF likely cannot be derived and analyzed by our methodology. However, we briefly explore the effect of distance and BRF signal acquisition and how the correlation between a BRF's peak-to-peak value and voltage changes with respect to distance. This is shown in Figure 10, in which we observe the correlation coefficient of peak-to-peak BRF values and voltage with respect to varying distance. We find that the correlation remains relatively constant with our methodology between 8 m and 32 m but appears to show a decrease in correlation for 40 m. While this analysis is inconclusive towards quantifying the effect of distance on signal quality for analytical purposes, we importantly note that future work will require quantitative analysis towards identifying the various factors and conditions that elucidate the limits and design trade-offs of this camera system.

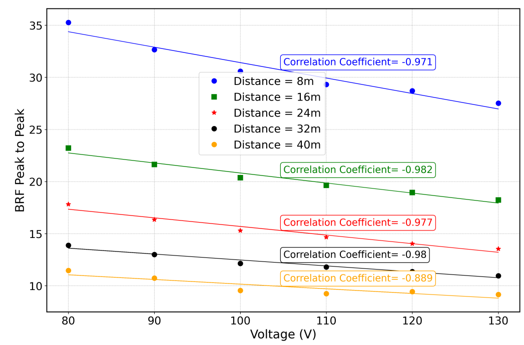

Figure 10: Correlation of a particular LED bulb's BRF, peak to peak value with respect to voltage. This experiment was conducted in a controlled, outdoor scene, in which we capture BRFs of a single bulb at varied distances and source voltages. Distances are chosen in 8 m increments from 8 m to 40 m, while varying the source voltage with a variable power supply between 80V to 130V; voltage is varied in addition to distance to observe how distance affects while changes in voltage occur as well. As this experiment was performed in a 60 Hz grid, we first calibrate the camera's fps to cater towards the grid frequency.

For other future work, we also propose the development of site-generalizable models that can be used for inference across different sites in lieu of site-specific systems. We also consider evaluating the system in observing multiple bulbs simultaneously within a large field of view. Additionally, transitioning from offline post-processing to real-time, online estimation of grid parameters would further enhance the system's utility.

8 Conclusions

The demands of the energy transition call for increased grid visibility to address the existing and resulting disruptions to electric grids, especially in emerging economies. In this work, we evaluate a distributed voltage monitoring technique that leverages camera images as a proxy to estimate voltages supplied to electric lights. Our findings show that statistical parameters, especially the maximum, minimum, mean, and peak-peak features of the bulb response functions, as highly indicative parameters exhibiting high absolute correlation with the voltage changes across bulbs and bulb types. We also describe a classification pipeline with the Random Forest models achieving accuracy of 91.4% and 94.9% in distinguishing normal voltage and sustained undervoltage voltage events for two separate in-situ deployment sites. We postulate that this system establishes and emphasizes the potential of image-based grid sensing of the voltage, which can enable widespread voltage quality indicator measurement efforts, thus enhancing attempts to enable quality electric service delivery, particularly in settings where scalable measurements are not prevalent.

Acknowledgments

We thank the U.S. National Science Foundation (Grant #1854133) and the Rockefeller Foundation (Grant #2021 PNC 010) for support.

References

[1] 2023. *Kenya Power Receives First Batch of 700,000 Smart Meters*. https://ntvkenya.co.ke/news/kenya-power-receivesfirst-batch-of-700000-smart-meters/

[2] ERA Uganda. 2018. Guidelines and Standards - ERA - Electricity Regulatory Authority. https://www.era.go.ug/index.php/resource-centre/regulatory-instruments/guidelines-and-standards

[3] IRENA. 2024. World Energy Transitions Outlook 2024. https://www.irena.org/Publications/2024/Nov/World-Energy-Transitions-Outlook-2024

[4] IDS Imaging. [n. d.]. UI-3860CP Rev. 2. https://en.ids-imaging.com/store/ui-3860cp-rev-2.html

[5] A. Acakpovi, R. Abubakar, N. Y. Asabere, and I. B. Majeed. 2019. Barriers and prospects of smart grid adoption in Ghana. *Procedia Manufacturing* 35 (2019), 1240–1249. doi:10.1016/j.promfg.2019.06.126

[6] Sustainable Energy Africa. 2015. Smart Metering: Overview and Considerations for South African Municipalities. https://africancityenergy.org/uploads/resource_127.pdf

[7] Basel Alsayyed, Yazan Alhaj, and Omar Alhaj. 2015. Review of power quality monitoring systems. *International Journal of Scientific & Engineering Research* 6, 9 (2015), 222–227.

[8] Susanna B. Berkouwer, Pierre E. Biscaye, Maya Mikdash, Steven L. Puller, and Catherine D. Wolfram. 2024. Improving Voltage Quality through Transformer Construction in Accra, Ghana. https://kleinmanenergy.upenn.edu/research/publications/improving-voltage-quality-through-transformer-construction-in-accra-ghana/

[9] S. Bhattacharyya, J. M. A. Myrzik, and W. L. Kling. 2007. Consequences of poor power quality - an overview. In *2007 42nd International Universities Power Engineering Conference*. 651–656. doi:10.1109/UPEC.2007.4469025

[10] Federica B. Bianco, Steven E. Koonin, Charlie Mydlarz, and Mohit S. Sharma. 2016. Hypertemporal Imaging of NYC Grid Dynamics: Short paper. In *Proceedings of the 3rd ACM International Conference on Systems for Energy-Efficient Built Environments (BuildSys '16)*. Association for Computing Machinery, New York, NY, USA, 61–64. doi:10.1145/2993422.2993570

[11] Moussa P Blimpo and Malcolm Cosgrove-Davies. 2019. Electricity Access in Sub-Saharan Africa. https://openknowledge.worldbank.org/bitstream/handle/10986/31333/9781464813610.pdf

[12] Joseph Breda and Jay Taneja. 2018. Fancy That: Measuring Electricity Grid Voltage Using a Phone and a Fan. In *Proceedings of the 1st ACM SIGCAS Conference on Computing and Sustainable Societies (COMPASS '18)*. Association for Computing Machinery, New York, NY, USA, 1–9. doi:10.1145/3209811.3209864

[13] I. Diahovchenko, M. Kolcun, Z. Conka, V. Savkiv, and R. Mykhailyshyn. 2020. Progress and challenges in smart grids: Distributed generation, smart metering, energy storage and smart loads. *Iranian Journal of Science and Technology, Transactions of Electrical Engineering* 44 (2020), 1319–1333. doi:10.1007/s40998-020-00322-8

[14] Gregory Dobler, Federica B. Bianco, Mohit S. Sharma, Andreas Karpf, Julien Baur, Masoud Ghandehari, Jonathan Wurtele, and Steven E. Koonin. 2021. The Urban Observatory: A Multi-Modal Imaging Platform for the Study of Dynamics in Complex Urban Systems. *Remote Sensing* 13, 8 (Jan. 2021), 1426. doi:10.3390/rs13081426 Number: 8 Publisher: Multidisciplinary Digital Publishing Institute.

[15] International Energy Agency. 2022. Africa Energy Outlook 2022: A World Energy Outlook Special Report. https://www.iea.org/reports/africa-energy-outlook-2022

[16] Jessica Kersey, Judith Mbabazi, Civian Kiki Massa, Lydia Letaru, June Lukuyu, Elena van Hove, and Paul Kyoma. 2023. Illuminating Energy Inequities in Informal Urban Communities: Main Findings Report. Main Findings Report.

[17] Samina Khalid, Tehmina Khalil, and Shamila Nasreen. 2014. A survey of feature selection and feature extraction techniques in machine learning. In *2014 Science and Information Conference*. 372–378. doi:10.1109/SAI.2014.6918213

[18] Noah Klugman, Joshua Adkins, Emily Paszkiewicz, Molly G. Hickman, Matthew Podolsky, Jay Taneja, and Prabal Dutta. 2021. Watching the Grid: Utility-Independent Measurements of Electricity Reliability in Accra, Ghana. In *Proceedings of the 20th International Conference on Information Processing in Sensor Networks (co-located with CPS-IoT Week 2021)*. ACM, Nashville TN USA, 341–356. doi:10.1145/3412382.3458276

[19] Noah Klugman, Joshua Adkins, Emily Paszkiewicz, Molly G. Hickman, Matthew Podolsky, Jay Taneja, and Prabal Dutta. 2021. Watching the Grid: Utility-Independent Measurements of Electricity Reliability in Accra, Ghana. In *Proceedings of the 20th International Conference on Information Processing in Sensor Networks (Co-Located with CPS-IoT Week 2021)* (Nashville, TN, USA) *(IPSN '21)*. Association for Computing Machinery, New York, NY, USA, 341–356. doi:10.1145/3412382.3458276

[20] Cable Labs. 2022. Gridmetrics Inc. https://gridmetrics.io/

[21] Xiaodan Lin, Yangfu Li, Jianqing Zhu, and Huanqiang Zeng. 2023. Deflicker-CycleGAN: Learning to Detect and Remove Flickers in a Single Image. *IEEE Transactions on Image Processing* 32 (2023), 709–720. doi:10.1109/TIP.2022.3231748 Conference Name: IEEE Transactions on Image Processing.

[22] D. Marr, E. Hildreth, and Sydney Brenner. 1997. Theory of edge detection. *Proceedings of the Royal Society of London. Series B. Biological Sciences* 207, 1167 (Jan. 1997), 187–217. doi:10.1098/rspb.1980.0020 Publisher: Royal Society.

[23] Civian Kiki Massa and Jay Taneja. 2023. Bridges to Nowhere: Electricity connections with poor power quality hamper growth. https://energyforgrowthhub.org/.

[24] David McCollum, Luis Gomez Echeverri, Keywan Riahi, and Simon Parkinson. 2017. Sdg7: Ensure access to affordable, reliable, sustainable and modern energy for all. (2017).

[25] Samuel B Miles, Molly G Hickman, Genevieve Flaspohler, Mohini Bariya, Jackson Mughuma, and Dan Kammen. 2023. Beyond Access: Measuring Power Quality Issues at 27 Healthcare Facilities in the DRC. (2023).

[26] B. Muriuki. 2023. *Kenya Power Goes for Smart Meters to Lock Out Power Cartels*. https://www.citizen.digital/news/kenya-power-goes-for-smartmeters-to-lock-out-power-cartels-n330881

[27] Kevin Murphy. 2022. *Probabilistic Machine Learning*. The MIT Press. https://mitpress.mit.edu/9780262046824/probabilistic-machine-learning/

[28] nLine Inc. 2024. POWERWATCH SENSOR TECHNICAL SPECIFICATIONS. https://nline.io/docs/powerwatch_spec_sheet.pdf.

[29] Olufolahan Osunmuyiwa and Margaret Odero. 2024. Leveraging Power Quality and Reliability Measurements for Electricity Equity and Justice in sub-Saharan Africa. https://blog.nline.io/pqr-for-energy-justice

[30] Przemysław Otomański, Grzegorz Wiczyński, and Bartosz Zając. 2017. Flicker Vision of Selected Light Sources. *Measurement Science Review* 17, 5 (Oct. 2017), 232–240. doi:10.1515/msr-2017-0028

[31] Hugo Le Picard. 2020. The Potential of Digital Technologies for Centralized Electricity Systems in Sub-Saharan Africa. https://www.ifri.org/sites/default/files/migrated_files/documents/atoms/files/le_picard_digital_technologies_africa_2021.pdf

[32] Philip W. T. Pong, Anuradha M. Annaswamy, Benjamin Kroposki, Yingchen Zhang, Ram Rajagopal, Gil Zussman, and H. Vincent Poor. 2021. Cyber-enabled grids: Shaping future energy systems. *Advances in Applied Energy* 1 (Feb. 2021), 100003. doi:10.1016/j.adapen.2020.100003

[33] A. Rihaczek. 1968. Signal energy distribution in time and frequency. *IEEE Transactions on Information Theory* 14, 3 (May 1968), 369–374. doi:10.1109/TIT.1968.1054157 Conference Name: IEEE Transactions on Information Theory.

[34] Daniel Sabin, Mathew Norwalk, Kevin Kittredge, and Steven Johnston. 2022. IEEE Power Quality Standards. In *2022 20th International Conference on Harmonics & Quality of Power (ICHQP)*. 1–6. doi:10.1109/ICHQP53011.2022.9808543 ISSN: 2164-0610.

[35] Zeal Shah, Alex Yen, Ajey Pandey, and Jay Taneja. 2019. GridInSight: Monitoring Electricity Using Visible Lights. In *Proceedings of the 6th ACM International Conference on Systems for Energy-Efficient Buildings, Cities, and Transportation*. ACM, New York NY USA, 243–252. doi:10.1145/3360322.3360855

[36] M. Sheinin, Y. Y. Schechner, and K. N. Kutulakos. 2017. Computational Imaging on the Electric Grid. In *Proceedings of the IEEE Conference on Computer Vision and Pattern Recognition*. 6437–6446.

[37] M. Sheinin, Y. Y. Schechner, and K. N. Kutulakos. 2018. Rolling Shutter Imaging on the Electric Grid. In *2018 IEEE International Conference on Computational Photography (ICCP)*. 1–12. doi:10.1109/ICCPHOT.2018.8368472

[38] Peter Twesigye. 2024. Understanding Electricity Utilities in Sub-Saharan Africa: The Role of Civil Society in Improving Performance, Governance, and Accountability. https://policy-practice.oxfam.org/resources/understanding-electricity-utilities-in-sub-saharan-africa-the-role-of-civil-soc-621616/

[39] Lexuan Xu, Guang Hua, Haijian Zhang, Lei Yu, and Ning Qiao. 2023. Seeing Electric Network Frequency From Events. In *Proceedings of the IEEE/CVF Conference on Computer Vision and Pattern Recognition (CVPR)*. 18016–18025.

[40] Jie Yang and Haochen Hua. 2020. Power Quality and Power Experience. In *Energy Internet: Systems and Applications*, Ahmed F Zobaa and Junwei Cao (Eds.). Springer International Publishing, Cham, 381–395. doi:10.1007/978-3-030-45453-1_13

[41] Alex Yen, Zeal Shah, Benjamin Ochoa, Pat Pannuto, and Jay Taneja. 2022. EffiSenseSee: towards classifying light bulb types and energy efficiency with camera-based sensing. In *Proceedings of the 9th ACM International Conference on Systems for Energy-Efficient Buildings, Cities, and Transportation (BuildSys '22)*. Association for Computing Machinery, New York, NY, USA, 69–78. doi:10.1145/3563357.3564062

[42] ZESCO. 2022. ZESCO POWER QUALITY MANAGEMENT SYSTEM. Presented at Unipower Power Quality Training 2022, Zambia.

[43] X. X. Zhu, S. Chen, F. Zhang, Y. Shi, and Y. Wang. 2025. GlobalBuildingAtlas: an open global and complete dataset of building polygons, heights and LoD1 3D models. *Earth System Science Data* 17, 12 (2025), 6647–6668. doi:10.5194/essd-17-6647-2025